Role of Amino-Terminal Residues in the Folding of the Constant Fragment of the Immunoglobulin Light Chain

Yuji Goto and Kozo Hamaguchi*

Department of Biology, Faculty of Science, Osaka University, Toyonaka, Osaka 560, Japan

Received August 7, 1986; Revised Manuscript Received November 13, 1986

ABSTRACT: Three constant fragments with different amino terminals, C_L(105–214), C_L(109–214), and C_L(113–214), were obtained by limited proteolysis with trypsin or papain of a type λ immunoglobulin light chain. The conformations of the three C_L fragments were indistinguishable on the basis of circular dichroism and tryptophyl fluorescence spectra. The stability to heat and guanidine hydrochloride of C_L(105–214) was almost the same as that of C_L(109–214), but the stability of C_L(113–214) was slightly lower than that of C_L(105–214) or C_L(109–214). The midpoint of the thermal unfolding transition at pH 7.5 was at 60.0 °C for C_L(105–214), 60.4 °C for C_L(109–214), and 57.5 °C for C_L(113–214). The midpoint of the unfolding transition by guanidine hydrochloride at pH 7.5 and 25 °C was 1.2 M for C_L(105–214) and C_L(109–214) and at 1.0 M for C_L(113–214). The kinetics of unfolding and refolding by guanidine hydrochloride of these C_L fragments were analyzed on the basis of the three-species mechanism, $U_1 \rightleftharpoons U_2 \rightleftharpoons N$, where U_1 and U_2 are the slow-folding and fast-folding species, respectively, of unfolded protein and N is native protein. It was found that only the microscopic unfolding rate constant for C_L(113–214) is 2–3 times greater than that for C_L(105–214) or C_L(109–214) and that the other microscopic rate constants for the three C_L fragments are all the same. These findings indicated that the amino-terminal residues, Gly-109–Lys-112, or a part of them, stabilize the C_L(113–214) fragment by decreasing only the unfolding rate, that the transition state of the folding of the C_L fragment is independent of the presence or absence of this peptide, and that, at the last step of folding, the peptide is incorporated into the globular domain, thus stabilizing it.

Each domain of the immunoglobulin molecule consists of about 110 amino acid residues and has only one intrachain disulfide bond buried in the interior hydrophobic region between two β-sheets (Beale & Feinstein, 1976; Amzel & Poljak, 1978). We have carried out a series of studies on the folding of the C_L fragment obtained by digestion with trypsin or papain of an immunoglobulin light-chain Nag of type λ (Azuma et al., 1978; Goto et al., 1979; Goto & Hamaguchi, 1979, 1981, 1982a,b, 1986a,b; Ashikari et al., 1984; Kikuchi et al., 1986). In earlier studies, we used the C_L(105–214)[1] fragment obtained by tryptic digestion of Nag protein. We then used the C_L(109–214) fragment obtained by papain digestion of Nag protein, because the yield of the latter C_L fragment was much higher than that obtained by tryptic digestion. Recently, we have found that, in addition to C_L(105–214), the C_L(113–214) fragment is also obtained by tryptic digestion of Nag protein. In Figure 1, the positions of cleavage by trypsin and papain are indicated by arrows on the crystal structure of the light chain of Fab (Kol) represented by the α-carbon backbone (Marquart et al., 1980).[2]

In the present experiments, we studied the folding equilibria and kinetics of the C_L(105–214) and C_L(113–214) fragments, obtained by tryptic digestion and the C_L(109–214) fragment obtained by papain digestion of Nag protein and attempted to clarify the role of the N-terminal residues in the folding of the C_L fragment. We found that although the CD and fluorescence spectra of these three C_L fragments are all the same, C_L(113–214) is slightly less stable to heat and Gdn-HCl than C_L(105–214) and C_L(109–214). The kinetics of unfolding and refolding were analyzed on the basis of the three-species mechanism (Brandts et al., 1975; Garel & Baldwin, 1975). It was found that only the microscopic unfolding rate constant for C_L(113–214) is 2–3 times greater than that for C_L(105–214) or C_L(109–214) and that the microscopic refolding rate constant and the rate constants for the interconversion between the two species in the unfolded state for the three C_L fragments are all the same. The lower stability of C_L(113–214) can be well explained only in terms of its greater unfolding rate. These findings indicate that the residues Gly-109–Lys-112, or a part of them, play an important role but that residues Leu-105–Leu-108 play no role in the folding of the C_L fragment. It was also suggested that the residues 109–112 stabilize the molecule at the last stage of folding.

Materials and Methods

Materials. Immunoglobulin light-chain Nag (type λ) was prepared from the urine of a multiple myeloma patient as described previously (Goto et al., 1979). In order to obtain the C_L fragment, Nag protein, in which the penultimate cysteine residue was alkylated with iodoacetamide, was digested with trypsin or papain. The C_L(109–214) fragment was obtained by papain digestion as described previously (Goto & Hamaguchi, 1979). The C_L(105–214) and C_L(113–214) fragments were obtained by tryptic digestion of Nag protein. In the final step of purification of the C_L fragment obtained by tryptic digestion, two peaks appeared by ion-exchange chromatography on a DEAE-cellulose column, and the protein contained in the first major peak was identified as C_L(105–214) (Goto et al., 1979). The protein contained in the second

[1] Abbreviations: CD, circular dichroism; Gdn-HCl, guanidine hydrochloride; SDS, sodium dodecyl sulfate; Tris, tris(hydroxymethyl)-aminomethane; C_L(109–214), fragment corresponding to sequence 109–214 obtained by papain digestion of type λ light chain (Nag); C_L(105–214) and C_L(113–214), fragments corresponding to sequences 105–214 and 113–214, respectively, obtained by tryptic digestion of type λ light chain (Nag); HPLC, high-performance liquid chromatography; DPPC, diphenylcarbamyl chloride.

[2] The numbering system used in this paper is based on type λ light chain (Kol) (Marquart et al., 1980).

0006-2960/87/0426-1879$01.50/0

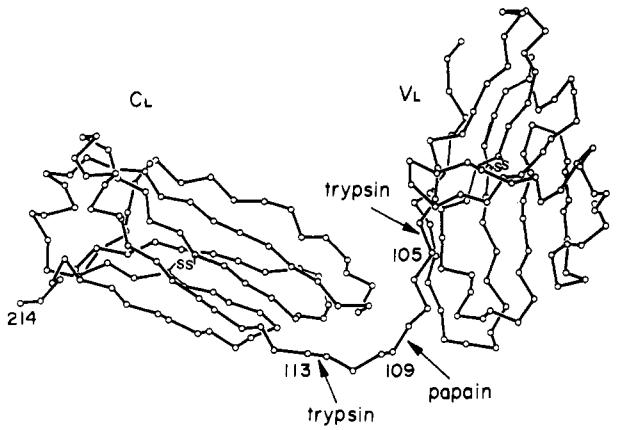

FIGURE 1: Crystal structure of the light chain of Fab(Kol) represented by the α-carbon backbone (Marquart et al., 1980). The arrows indicate the peptide bonds cleaved by trypsin and papain. The locations of the intrachain disulfide bonds are also indicated.

minor peak was pure on the basis of polyacrylamide gel electrophoresis in both the presence and absence of SDS. The amino-terminal sequence of the protein was determined by manual Edman degradation to be Ala-Ala-Pro, which corresponds to the sequence from residues 113–115 on the basis of the sequence of the $C_L(\lambda)$ domain (Marquart et al., 1980). The amino acid composition of this protein was as expected for the sequence of 113–214, and the penultimate cysteine residue was detected as (carboxymethyl)cysteine. Thus, the protein contained in the minor peak was identified as the C_L(113–214) fragment, the yield of which was about 30% of the major C_L(105–214).

Gdn-HCl (specially purified grade) was obtained from Nakarai Chemicals. Bovine pancreatic trypsin (DPCC-treated, type XI) and papain (type III) were obtained from Sigma.

CD Measurements. Measurements were carried out in 50 mM Tris-HCl buffer containing 0.15 M NaCl at pH 7.5 and at 25 °C. A 10 mM sodium phosphate buffer at pH 7.5 containing 0.15 M NaCl was used for measurements of thermal unfolding.

The CD spectra of the C_L fragments were measured with a Jasco spectrophotometer, Model J-500a, equipped with a DP-501 data processor. The details of the CD measurements have been described previously (Goto & Hamaguchi, 1986a). Thermal unfolding of the C_L fragments was measured in terms of the ellipticity at 218 nm. The protein concentration was 0.2 mg/mL, and a 0.2-cm cell was used. The temperature was increased continuously at a rate of 0.5 °C/min and was monitored with a calibrated copper–constantan thermocouple. The unfolding transition curves were all the same when the temperature was increased with rates below 0.5 °C/min. The reversibility was examined by measuring CD at 218 nm after lowering the temperature to 20 °C at a rate of 2 °C/min from the thermally unfolded state.

Fluorescence Measurements. Fluorescence spectra were measured with a Hitachi fluorescence spectrophotometer, Model MPF-4, equipped with a spectral corrector. Tryptophyl fluorescence was measured by using 280-nm light for excitation. The protein concentration was about 0.02 mg/mL. The temperature was maintained at 25 °C with a thermostatically controlled cell holder.

Kinetic Measurements. Unfolding and refolding reactions were measured on a Union Giken stopped-flow spectrophotometer, Model RA-401, using fluorescence detection. The details of the apparatus have been described previously (Goto & Hamaguchi, 1982a). The excitation wavelength was set at 280 nm, and fluorescence at wavelengths longer than 330 nm was observed. The reservoir and the observation cell were thermostated by circulating water at 25 °C. The final protein concentration was about 0.02 mg/mL.

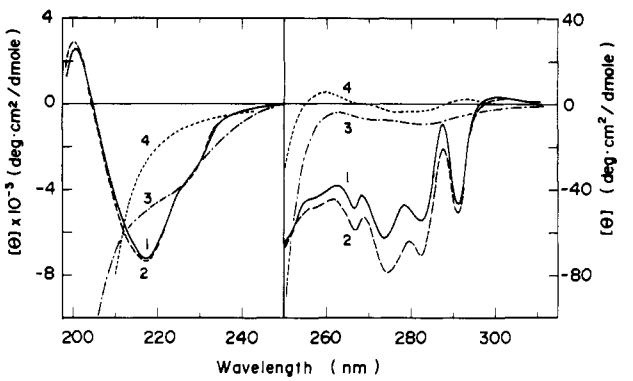

FIGURE 2: CD spectra of C_L(105–214) and C_L(113–214). (1) C_L(105–214) at 25 °C; (2) C_L(113–214) at 25 °C; (3) C_L(105–214) at 80 °C; (4) C_L(105–214) in the presence of 4 M Gdn-HCl at 25 °C.

The unfolding was initiated by mixing a C_L fragment solution with Gdn-HCl solution at a given concentration in a 1:1 ratio.

For the measurements of fast-refolding reactions, we used a pH jump to initiate the refolding. The initial unfolding conditions were pH 2.0 and 0.6 M Gdn-HCl. The protein solution was mixed with 0.2 M Tris-HCl buffer at pH 8.0 containing Gdn-HCl at a given concentration in a 1:1 ratio to give a final pH of 7.5. Refolding reactions were also measured with the Hitachi fluorescence spectrophotometer by dilution of Gdn-HCl concentration at pH 7.5. The refolding was initiated by manually mixing 0.1 mL of a C_L fragment solution in 4 M Gdn-HCl at pH 7.5 with 2.5 mL of a diluent containing Gdn-HCl at a given concentration at pH 7.5. The final protein concentration was 0.02 mg/mL.

All the kinetic data were analyzed as described previously (Goto & Hamaguchi, 1982a).

Amino Acid Analysis. The amino acid compositions of the C_L fragments were determined with an Irica amino acid analyzer, Model A-5500 (Kyoto, Japan). The samples were hydrolyzed in evacuated, sealed tubes with 6 N HCl at 110 °C for 24 h. The amino-terminal sequence of the C_L(113–214) fragment was determined by manual Edman degradation (Blombäck et al., 1966), and the phenylthiohydantoin derivatives of amino acids were identified by HPLC (Zimmerman et al., 1977) or thin-layer chromatography.

Polyacrylamide Gel Electrophoresis. Polyacrylamide gel electrophoresis on 15% gels in the presence of SDS was carried out according to the method described by Weber and Osborn (1969). Polyacrylamide gel electrophoresis on 7.5% gels in the absence of SDS was carried out according to the method described by Davis (1964).

Protein Concentration. Protein concentration was determined spectrophotometrically. The absorption coefficients at 280 nm for a 1% (w/v) solution in a 1.0-cm cell ($A^{1\%}_{1cm}$) of the three C_L fragments were assumed to be the same, and a value of 14.6 (Karlsson et al., 1972) was used.

pH Measurements. pH was measured with a Radiometer PHM 26c at 25 °C.

RESULTS

Conformation of the C_L Fragment. Figure 2 shows the CD spectra of the C_L(105–214) and C_L(113–214) fragments in Tris-HCl buffer at pH 7.5 and 25 °C. These CD spectra showed a minimum at 218 nm which is characteristic of the

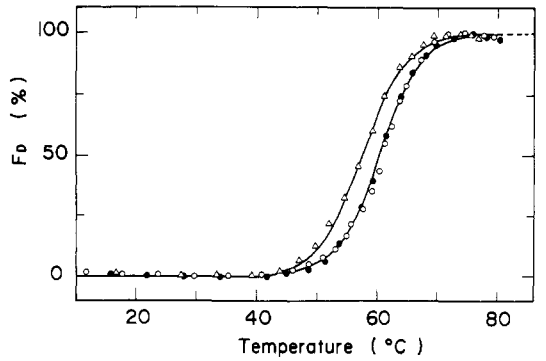

FIGURE 3: Thermal unfolding transition of C_L(105–214) (●), C_L(109–214) (○), and C_L(113–214) (△) at pH 7.5. The solid lines indicate the theoretical curves for C_L(105–214) and C_L(113–214) calculated by using the parameters shown in Table I. The ordinate represents the fraction of unfolded protein.

Table I: Thermodynamic Parameters and Transition Midpoints for the Thermal Unfolding of C_L Fragments at pH 7.5[a]

	T_m (°C)	ΔH at T_m (kcal/mol)	ΔS at T_m (eu)	ΔG_D at 60 °C (kcal/mol)
C_L(105–214)	60.0 ± 0.4	67.3 ± 1.8	202 ± 5	0
C_L(109–214)	60.4 ± 0.1	66.9 ± 0.4	201 ± 1	0.1
C_L(113–214)	57.5 ± 0.1	61.7 ± 2.2	187 ± 7	−0.5

[a] T_m is the temperature at the midpoint of the unfolding transition. The thermal transition curve was analyzed by assuming the two-state approximation of N (native) ⇌ D (unfolded), and the equilibrium constant of unfolding (K_D = [D]/[N]) was determined by the equation $K_D = f_D/(1 - f_D)$, where f_D is the fraction of the unfolded molecule at each temperature. ΔH at T_m was determined by the van't Hoff plot. Values are the average of three measurements.

β-sheet conformation. The spectrum of C_L(105–214) was the same as that of C_L(113–214) except for a small difference in the aromatic absorption region. The spectrum of C_L(109–214) was the same as that of C_L(105–214).

We measured the tryptophyl fluorescence of the three C_L fragments in Tris-HCl buffer at pH 7.5 and 25 °C. The spectra were all the same and had a maximum at 325 nm (Goto & Hamaguchi, 1979; Figure 2). The intensity at the maximum was 35% relative to the intensity in the presence of 4 M Gdn-HCl. The identity of the CD and fluorescence spectra of the three C_L fragments shows that their conformations are very similar.

Thermal Unfolding. In order to study the effect on the thermal stability of the N-terminal portion of the C_L fragment, we measured the thermal unfolding transitions of C_L(105–214), C_L(109–214), and C_L(113–214). Figure 2 shows the CD spectrum of C_L(105–214) at 80 °C and the spectrum in 4 M Gdn-HCl. The CD spectra of the thermally unfolded C_L(109–214) and C_L(113–214) were the same as that of the thermally unfolded C_L(105–214). The CD spectra of C_L(105–214), C_L(109–214), and C_L(113–214) in 4 M Gdn-HCl were the same. However, the spectra of the thermally unfolded C_L fragments were different from the spectra of the C_L fragments unfolded by 4 M Gdn-HCl. Figure 3 shows the thermal unfolding curves of these three C_L fragments measured in terms of the ellipticity at 218 nm. The thermal unfolding was almost completely (more than 90%) reversible. Cooperative transitions were observed. The unfolding transition curves of C_L(105–214) and C_L(109–214) were almost the same and had midpoints of transition at 60.0 and 60.4 °C, respectively (Table I). The C_L(113–214) fragment was slightly but evidently less stable than the other two C_L fragments and had a midpoint at 57.5 °C. The thermodynamic parameters for the thermal unfolding estimated by assuming the two-state transition are summarized in Table I.

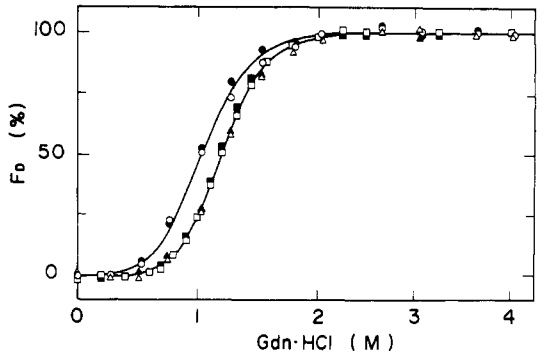

FIGURE 4: Unfolding transitions by Gdn-HCl of C_L(105–214) (triangles), C_L(109–214) (squares), and C_L(113–214) (circles) at pH 7.5 and 25 °C. The ordinate represents the fraction of unfolded protein. Unfolding transitions measured in terms of the ellipticity at 218 nm and the fluorescence at 350 nm are represented by open and closed symbols, respectively. Excitation wavelength for the fluorescence measurement was 295 nm. The solid lines indicate the theoretical curves for C_L(105–324) and C_L(113–214) constructed by using the equation proposed by Tanford (1970) (see the footnote of Table II) and the values of $\Delta G_D^{H_2O}$ and Δn obtained on the basis of CD data (Table II).

Table II: Free Energy Changes of Unfolding by Gdn-HCl and Transition Midpoints for C_L Fragments at pH 7.5 and 25 °C[a]

	C_m (M)	$\Delta G_D^{1.2M}$ (kcal/mol)	$\Delta G_D^{H_2O}$ (kcal/mol)	Δn	method
C_L(105–214)	1.2	0	5.7	29.0	CD
	1.2	0	5.7	29.2	fluorescence
C_L(109–214)	1.2	0	5.7	29.5	CD
	1.2	0	5.6	29.4	fluorescence
C_L(113–214)	1.0	−0.5	4.6	26.2	CD
	1.0	−0.5	4.5	26.2	fluorescence

[a] C_m is the concentration of Gdn-HCl at the midpoint of the unfolding transition. The transition curves were analyzed by assuming the two-state approximation of N (native) ⇌ D (unfolded). The equilibrium constant of unfolding (K_D) was determined by $K_D = f_D/(1 - f_D)$ at each concentration of Gdn-HCl. $\Delta G_D^{1.2M}$ is the free energy change of unfolding at 1.2 M Gdn-HCl. $\Delta H_D^{H_2O}$ is the free energy change of unfolding is the absence of Gdn-HCl and was obtained by the equation proposed by Tanford (1970), $\Delta G_D = \Delta G_D^{H_2O} - \Delta nRT \ln(1 + ka_\pm)$, where Δn is the difference in the number of binding sites between unfolded and folded states, k is the average binding constant of the sites, and $a_\pm$ is the mean ion activity of Gdn-HCl. We used 0.6 M^{-1} as the value of k [Pace & Vanderburg, 1979; see Goto and Hamaguchi (1979)].

Unfolding by Gdn-HCl. Figure 4 shows the unfolding transitions by Gdn-HCl of the three C_L fragments. These unfolding transitions were found to be reversible [see also Figure 1 in Goto and Hamaguchi (1982a)]. The unfolding transition curve measured in terms of the ellipticity at 218 nm was the same as the curve measured in terms of the fluorescence at 350 nm. As was the case for thermal unfolding, C_L(113–214) was less stable to Gdn-HCl than C_L(105–214) and C_L(109–214) and had a midpoint of unfolding at 1.0 M Gdn-HCl. The transition curves of C_L(105–214) and C_L(109–214) were the same and had a midpoint at 1.2 M Gdn-HCl. The free energy changes of unfolding in the absence of Gdn-HCl were estimated by using the equation proposed by Tanford (1970) on the basis of a Gdn-HCl binding model (Table II). The free energy change (4.6 kcal/mol) for C_L(113–214) was smaller than the free energy change (5.7 kcal/mol) for C_L(105–214) or C_L(109–214).

Unfolding Kinetics. In order to understand the difference in stability to Gdn-HCl, we measured the kinetics of unfolding and refolding by Gdn-HCl of the three C_L fragments at 25 °C. The kinetics of C_L(109–214) had already been studied in detail, and most of the data for C_L(109–214) are cited from

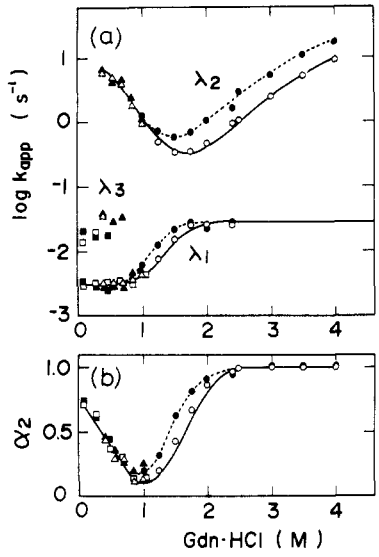

FIGURE 5: Dependence on Gdn-HCl concentration of (a) the apparent rate constants (λ_1, λ_2, and λ_3) and (b) the relative amplitude (α_2) of the fast phase for unfolding and refolding kinetics of C_L(105–214) (open symbols) and C_L(113–214) (closed symbols) at pH 7.5 and 25 °C. (○, ●) From unfolding kinetics obtained by stopped-flow measurements; (△, ▲) from refolding kinetics measured by stopped-flow fluorescence change when the pH was changed from 2.0 to 7.5; (□, ■) from refolding kinetics measured by the fluorescence change at 350 nm when the concentration of Gdn-HCl was changed from 4 M to lower concentrations at pH 7.5 by manual mixing. The initial concentrations of Gdn-HCl and protein for the stopped-flow unfolding measurements were 0 M and 0.04 mg/mL, respectively. Initial conditions for the stopped-flow refolding measurements were 0.04 mg/mL protein and 0.6 M Gdn-HCl at pH 2.0, and final conditions were 0.02 mg/mL protein and a desired concentration of Gdn-HCl at pH 7.5. Initial conditions for the refolding measurements by manual mixing were about 1 mg/mL protein in 4 M Gdn-HCl at pH 7.5, and final conditions were 0.03 mg/mL protein and a desired concentration of Gdn-HCl at pH 7.5. The solid lines indicate the values for C_L(109–214) cited from a previous paper (Goto & Hamaguchi, 1982a).

our previous paper (Goto & Hamaguchi, 1982a).

As was the case for C_L(109–214) (Goto & Hamaguchi, 1982a), the unfolding kinetics of C_L(105–214) and C_L(113–214) inside the transition zone (1–2 M Gdn-HCl) could be described in two-exponential terms:

$$F(t) - F(\infty) = F_1 \exp(-\lambda_1 t) + F_2 \exp(-\lambda_2 t) \qquad (1)$$

where λ_1 and λ_2 are the apparent rate constants of the slow and fast phases, respectively, and F_1 and F_2 are the amplitudes of the respective phases. The amplitudes of the slow and fast phases relative to the total fluorescence change are described by α_1 and α_2, respectively, where $\alpha_1 + \alpha_2 = 1$. Figure 5 shows the dependence of the kinetic parameters of unfolding of the three C_L fragments on the final concentration of Gdn-HCl. The relative amplitude of the fast phase increased greatly with the increase in the concentration of Gdn-HCl, and the total change in the fluorescence above 2.5 M Gdn-HCl could be expressed as a first-order process.

The unfolding kinetics of C_L(105–214) were identical with those of C_L(109–214). On the other hand, the unfolding of C_L(113–214) was evidently faster than that of C_L(105–214) or C_L(109–214) (Figure 5). The apparent rate constant for the fast phase of C_L(113–214) was 2–3 times larger than that for C_L(105–214) or C_L(109–214). The changes with Gdn-HCl concentration of the apparent rate constant (λ_1) of the slow phase and of the amplitude (α_2) of the fast phase for C_L(113–214) were similar to those of C_L(105–214) or C_L(109–214), except that the transition was shifted by 0.2 M to a lower concentration range of Gdn-HCl.

Refolding Kinetics. In previous studies (Goto & Hamaguchi, 1982a), the fast-refolding kinetics of C_L(109–214) were measured by stopped-flow mixing of unequal volumes of protein in 2.5 M Gdn-HCl and diluent. In the present experiments, we measured the kinetics of refolding of the C_L fragment by stopped-flow mixing of protein in 0.6 M Gdn-HCl at pH 2.0, where the protein is denatured, with an equal volume of 0.2 M Tris-HCl buffer at pH 8.0 containing Gdn-HCl at a given concentration to give a final pH of 7.5. Using C_L(109–214), we confirmed that the parameters of the refolding kinetics obtained by the pH jump from 2.0 to 7.5 are the same as those obtained by dilution of Gdn-HCl from 2.5 M to a lower concentration. This shows that the refolding kinetics of the C_L fragment do not depend on whether it is unfolded by Gdn-HCl or by acid beforehand.

The dependence on Gdn-HCl concentration of the kinetic parameters of refolding is shown in Figure 5. It can be seen that the refolding kinetics of these three C_L fragments are all the same. A third phase appeared in the refolding kinetics for the three C_L fragments below 0.8 M Gdn-HCl. The apparent rate constant of the fast phase (λ_2), that of the slow phase (λ_1), and the relative amplitude of the fast phase (α_2) obtained from the refolding kinetics agreed well with the respective parameters obtained from the unfolding kinetics at around 1 M Gdn-HCl (Figure 5). The apparent rate constant of the additional phase was 5–10 times larger than that of the slow phase, but the relative amplitude of this phase was small (less than 10%). Thus, we did not take into account this additional phase further in the analysis of the folding kinetics [see Goto and Hamaguchi (1982a)]. The apparent rate constant of the fast phase increased with decreasing concentration of Gdn-HCl, while the apparent rate constant of the slow phase was constant below 0.8 M Gdn-HCl. The relative amplitude of the fast phase increased sharply below 0.8 M Gdn-HCl.

Discussion

We have described the unfolding and refolding of the three C_L fragments whose N-terminal portions each differ in length by four residues. The conformations of the C_L fragments were very similar, indicating that at least the residues from 105 to 112 are not essential for maintaining the global conformation of the C_L fragment. The measurements of unfolding equilibria with heat and Gdn-HCl showed that C_L(113–214) is slightly but distinctly less stable than C_L(105–214), while C_L(109–214) is as stable as C_L(105–214). The measurements of unfolding and refolding kinetics with Gdn-HCl showed that C_L(113–214) unfolds faster than C_L(109–214), while the unfolding kinetics of C_L(109–214) are the same as those of C_L(105–214), and that all three C_L fragments refold with the same kinetics. These findings indicate that the N-terminal residues from 109 to 112 are concerned with the rate-limiting step of the unfolding kinetics but not with the rate-limiting step of the refolding kinetics of the C_L fragment. In order to understand the role of the N-terminal residues in the folding of the C_L fragment, we analyzed the kinetic parameters (Figure 5) to obtain the microscopic rate constants.

As described previously (Goto & Hamaguchi, 1982a), the unfolding and refolding kinetics of C_L(109–214) above 1.0 M Gdn-HCl can be explained on the basis of the following mechanism:

$$U_1 \underset{k_{21}}{\overset{k_{12}}{\rightleftharpoons}} U_2 \underset{k_{32}}{\overset{k_{23}}{\rightleftharpoons}} N \qquad (2)$$

where N is native protein, U_1 and U_2 are the slow-folding and fast-folding species, respectively, of unfolded protein, and k_{12},

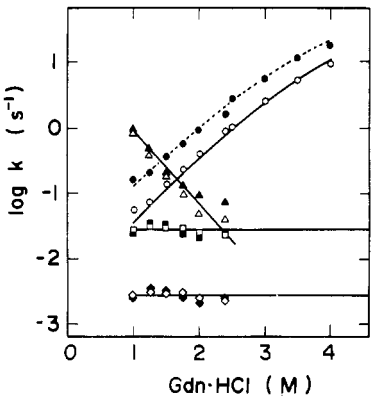

FIGURE 6: Dependence of Gdn-HCl concentration of the microscopic rate constants estimated on the basis of eq 2 for folding of C_L(105–214) (open symbols) and C_L(113–214) (closed symbols) at pH 7.5 and 25 °C. (△, ▲) k_{23}; (○, ●) k_{32}; (□, ■) k_{21}; (◇, ◆) k_{12}. The solid lines indicate the values for C_L(109–214) cited from the previous paper (Goto & Hamaguchi, 1982a).

k_{21}, k_{23}, and k_{32} are the rate constants of the respective processes. The equilibrium between U_1 and U_2 was independent of the concentration of Gdn-HCl, and K_{21} ($=k_{21}/k_{12}$) was 10, about 90% of the unfolded protein being the slow-folding species. In the refolding kinetics below 1.0 M Gdn-HCl, α_2 increased with decreasing concentration of Gdn-HCl. This could not be explained only on the basis of eq 2, but the following mechanism, in which intermediate I is involved, had to be used (Goto & Hamaguchi, 1982a):

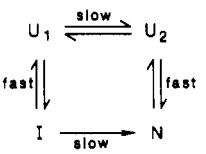

(3)

where the stability of I, which is in rapid equilibrium with U_1, increases with decreasing concentration of Gdn-HCl.

As shown in Figure 5, the kinetic parameters for C_L(105–214) were the same as those for C_L(109–214). This indicates that the folding mechanism of C_L(105–214) is the same as that of C_L(109–214) and that residues 105–108 are not concerned in the unfolding and refolding of the C_L fragment. The kinetic parameters for C_L(113–214) were similar to those for C_L(109–214), except that the changes with Gdn-HCl concentration in the values of λ_1, λ_2, and α_2 under the unfolding conditions shift to a lower concentration of Gdn-HCl. This indicates that the unfolding and refolding of C_L(113–214) can also be explained in the same way as described above. We analyzed the kinetic parameters for C_L(105–214) and C_L(113–214) above 1.0 M Gdn-HCl on the basis of eq 2, in which the value of K_{21} is independent of the concentration of Gdn-HCl, and estimated the microscopic rate constants. In this analysis, we assumed the value of K_{21} to be the same as the value (10) for C_L(109–214).

The microscopic rate constants thus obtained were plotted against Gdn-HCl concentration as shown in Figure 6. Table III shows the microscopic rate constants in the presence of 1.25 M Gdn-HCl. All the values for C_L(105–214) agree well with the values for C_L(109–214). The rate constants for the interconversion between U_1 and U_2 for C_L(113–214) are the same as those for C_L(109–214), indicating that the interconversion in the unfolded state is independent of the N-terminal portion 105–112. Previously, we assumed that the two forms of the unfolded species of C_L(109–214) occur owing to cis–trans isomerization of Pro-143 which is cis in the folded state (Goto & Hamaguchi, 1982a). Since Pro-111 is contained in

Table III: Microscopic Rate Constants of the Unfolding and Refolding of C_L Fragments in 1.25 M Gdn-HCl on the Basis of Equation 2 at pH 7.5 and 25 °C[a]

	k_{12} (s^{-1})	k_{21} (s^{-1})	k_{23} (s^{-1})	k_{32} (s^{-1})	f_D	$\Delta G_D^{1.25M}$ (kcal/mol)
C_L(105–214)	0.0031	0.031	0.38	0.072	0.68 (0.58)	−0.4 (−0.2)
C_L(109–214)	0.0033	0.033	0.47	0.056	0.57 (0.57)	−0.2 (−0.2)
C_L(113–214)	0.0033	0.033	0.45	0.190	0.82 (0.76)	−0.9 (−0.7)

[a] f_D and $\Delta G_D^{1.25M}$ are the values calculated from the microscopic rate constants. Values in parentheses are the observed values.

Scheme I

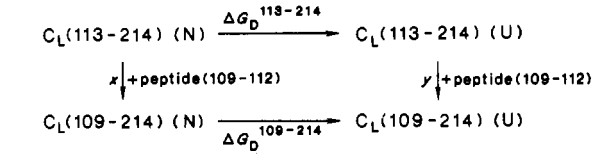

C_L(105–214) and C_L(109–214) but not in C_L(113–214), it cannot be responsible for the appearance of the slow phase. While the microscopic refolding rate constants of the three C_L fragments are all the same, only the microscopic unfolding rate constants from U_2 to N for C_L(113–214) is 2–3 times larger than that for C_L(105–214) or C_L(109–214). The fraction of native protein (f_N) is given by $k_{12}k_{23}/\lambda_1\lambda_2$, and the free energy change of unfolding is obtained by using the equation $\Delta G_D = -RT \ln (1 - f_N)/f_N$. The calculated values of f_D ($=1 - f_N$) and ΔG_D for the three C_L fragments in 1.25 M Gdn-HCl are in good agreement with the observed values (Table III). This indicates the validity of the analysis described above. It is shown that the difference in the free energy change of unfolding between C_L(113–214) and C_L(105–214) [or C_L(109–214)] (about 0.5 kcal/mol at 1.25 M Gdn-HCl) is explained only in terms of the difference in the microscopic unfolding rate constant between these C_L fragments. The low stability to heat of C_L(113–214) compared with that of C_L(109–214) or C_L(105–214) may also be explained only in terms of the difference in the thermal unfolding rate constant. The difference in the free energy change in the absence of Gdn-HCl between C_L(113–214) and C_L(109–214) [or C_L(105–214)] is estimated to be 1.0 kcal/mol (Table II). This value is larger by 0.5 kcal/mol than the value in the presence of 1.25 M Gdn-HCl. However, the two values may be regarded as consistent, because the values of the free energy change obtained by extrapolation to zero concentration of Gdn-HCl involve a rather large error (Pace, 1986).

The following scheme (Scheme I) will be helpful in understanding the difference in the stability between C_L(113–214) and C_L(109–214). In this cycle, the relation $\Delta G_D^{113-214} + y = \Delta G_D^{109-214} + x$ holds, where $\Delta G_D^{109-214}$ and $\Delta G_D^{113-214}$ are the free energy changes of unfolding of C_L(109–214) and C_L(113–214), respectively, y is the free energy change of linking the peptide (109–112) to C_L(113–214) in the unfolded state, and x is the free energy change of linking the peptide (109–112) to C_L(113–214) in the native state. x may be written as the sum of y and the free energy change of interaction of the peptide with the C_L(113–214) portion (ΔG_{inter}) in the native state, $x = y + \Delta G_{inter}$. In the absence of Gdn-HCl, $\Delta G_D^{113-214}$ and $\Delta G_D^{109-214}$ were estimated to be 4.6 and 5.6 kcal/mol, respectively (Table II). Thus, the free energy change of the interaction of the peptide (109–112) with the native C_L(113–214) (ΔG_{inter}) is estimated to be −1.0 kcal/mol, indicating that the presence of the peptide contributes to the stability of C_L(109–214) by 1.0 kcal/mol.

The kinetic results give us some insight into the folding pathway of the C_L fragment. We constructed the free energy

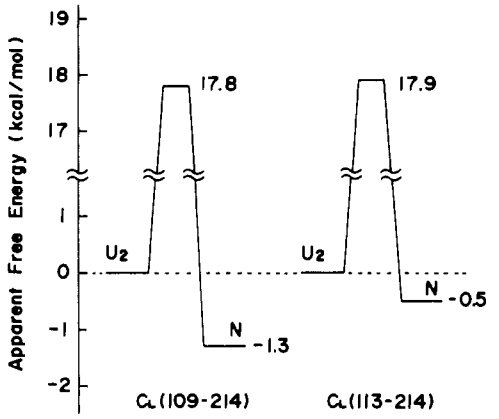

FIGURE 7: Free energy profiles for the unfolding and refolding of C_L(105–214) and C_L(113–214) in the presence of 1.25 M Gdn-HCl at pH 7.5 and 25 °C. N and U_2 represent the folded and unfolded states, respectively. The profiles were constructed by setting the unfolded state of C_L(105–214) and C_L(113–214) at the same energy level.

diagrams of the folding and unfolding transitions between U_2 and N (eq 2) for C_L(109–214) and C_L(113–214) at 1.25 M Gdn-HCl which is near the midpoint of the unfolding transition. The transition-state free energy, $\Delta G^{\ddagger}$, is calculated by using the relation

$$\Delta G^{\ddagger} = -RT \ln (kh/k_B T) \quad (4)$$

where k is the rate constant, h is Planck's constant, k_B is Boltzmann's constant, T is the temperature in kelvin, and R is the gas constant.

Figure 7 shows the free energy profiles for C_L(109–214) and C_L(113–214) constructed by setting the unfolded states for both proteins at the same energy level. Because the free energy change of linking the peptide (109–112) (y in the above cycle) in the unfolded state is the same as that in the native state and y does not contribute to the conformational free energy, the energy levels for these C_L fragments in the unfolded state are assumed to be the same. The profile for C_L(105–214) is the same as that for C_L(109–214). On this assumption, the free energy level of C_L(109–214) is lower by 0.8 kcal/mol than that of C_L(113–214) in the folded state, indicating that N-terminal residues 109–112 have a role of stabilizing the folded state. This value is near that obtained by the equilibrium measurements (0.5 kcal/mol). The energy levels of the transition states for both proteins are the same. This indicates that the N-terminal residues 109–112 stabilize the folded state only after the protein has passed its transition state of folding.

In previous papers (Goto & Hamaguchi, 1982a,b), we compared the unfolding and refolding kinetics of the reduced C_L(109–214) fragment, in which the intrachain disulfide bond is reduced, with those of the intact C_L(109–214) fragment. The reduced C_L fragment assumes a conformation very similar to the intact C_L fragment, although the stability of the former is lower than that of the latter owing to the larger conformational entropy of the former in the unfolded state (Goto & Hamaguchi, 1979). The microscopic refolding rate constant for the reduced C_L fragment is about 100 times smaller than that for the intact C_L fragment, while the microscopic unfolding rate constants for the two proteins differ only slightly. This shows that the transition state of folding is affected to the same extent as the native conformation by the presence of the disulfide bond. This is consistent with the idea that the transition state of folding is located near the folded conformation if the folding is measured by its compactness (Segawa & Sugihara, 1984a,b; Goldenberg & Creighton, 1985). The present results give additional information on the folding pathway of the C_L fragment and show that the stabilization of the domain by the N-terminal residues occurs only after the protein passes over its transition state, in which major interactions stabilizing the folded conformation are acquired. From the present results alone, we are unable to define which of the four residues (Ser-109-Gln-Pro-Lys-112) is (are) important for stabilizing the C_L domain. It is likely, however, that Lys-112 or Pro-111 located near the globular C_L(113–214) portion is more important than Gln-110 or Ser-109 which protrudes beyond the C_L portion.

REFERENCES

Amzel, L. M., & Poljak, R. L. (1979) *Annu. Rev. Biochem. 48*, 961–997.

Ashikari, Y., Arata, Y., & Hamaguchi, K. (1985) *J. Biochem. (Tokyo) 97*, 517–528.

Azuma, T., Kobayashi, O., Goto, Y., & Hamaguchi, K. (1978) *J. Biochem. (Tokyo) 83*, 1485–1492.

Beale, D., & Feinstein, A. (1976) *Q. Rev. Biophys. 9*, 135–180.

Blombäck, B., Blombäck, M., Edman, P., & Hessel, B. (1966) *Biochim. Biophys. Acta 115*, 371–396.

Brandts, H. F., Halvorson, H. R., & Brennan, M. (1975) *Biochemistry 14*, 4953–4963.

Chen, B. L., & Poljak, R. J. (1974) *Biochemistry 13*, 1295–1302.

Davis, B. J. (1964) *Ann. N.Y. Acad. Sci. 121*, 404–427.

Garel, J.-R., & Baldwin, R. L. (1975) *J. Mol. Biol. 94*, 611–620.

Goldenberg, D., & Creighton, T. E. (1985) *Biopolymers 12*, 2521–2537.

Goto, Y., & Hamaguchi, K. (1979) *J. Biochem. (Tokyo) 86*, 1433–1441.

Goto, Y., & Hamaguchi, K. (1981) *J. Mol. Biol. 146*, 321–340.

Goto, Y., & Hamaguchi, K. (1982a) *J. Mol. Biol. 156*, 891–910.

Goto, Y., & Hamaguchi, K. (1982b) *J. Mol. Biol. 156*, 911–926.

Goto, Y., & Hamaguchi, K. (1986a) *Biochemistry 25*, 2821–2828.

Goto, Y., & Hamaguchi, K. (1986b) *J. Biochem. (Tokyo) 99*, 1501–1511.

Goto, Y., Azuma, T., & Hamaguchi, K. (1979) *J. Biochem. (Tokyo) 85*, 1427–1438.

Karlsson, F. A., Peterson, P. A., & Berggård, I. (1972) *J. Biol. Chem. 247*, 1065–1073.

Kikuchi, H., Goto, Y., & Hamaguchi, K. (1986) *Biochemistry 25*, 2009–2013.

Marquart, M., Deisenhofer, J., Huber, R., & Palm, W. (1980) *J. Mol. Biol. 141*, 369–391.

Pace, C. N. (1986) *Methods Enzymol. 131*, 266–280.

Pace, C. N., & Vanderburg, K. E. (1979) *Biochemistry 18*, 288–292.

Segawa, S., & Sugihara, M. (1984a) *Biopolymers 23*, 2473–2488.

Segawa, S., & Sugihara, M. (1984b) *Biopolymers 23*, 2489–2498.

Tanford, C. (1970) *Adv. Protein Chem. 24*, 1–95.

Weber, K., & Osborn, M. (1969) *J. Biol. Chem. 244*, 4406–4412.

Zimmerman, C. L., Anella, E., & Pisano, J. J. (1977) *Anal. Biochem. 77*, 569–573.